Seismic stacking methods: hyperbolic and non-hyperbolic traveltime approximations

Pedro Chira-Oliva*, IECOS/UFPA and João Carlos R. Cruz, IG/UFPA

Abstract

The simulation of a zero-offset (ZO) from multicoverage seismic data is one of the main steps of the standard seismic processing. To obtain a ZO seismic trace there are several stacking methods using different kinds of traveltime approximations. The normal-moveout/dip-moveout (NMO/DMO) method is the more known in the geophysical literature. It is based on the stacking of reflection seismic data along a hyperbolic traveltime approximation, which is determined by stacking velocity analysis in the offset domain. To simulate a ZO seismic section there exist different traveltime approximations whose accuracy depends on the offset and reflector curvature. Stacking methods, e.g. Common-Reflection-Surface (CRS) and Multifocusing (MF) extend conventional stacking of seismic traces over offset to multidimensional stacking over offset-midpoint. By using hyperbolic or non-hyperbolic traveltime formulas, these methods depend on three parameters and approximate the kinematic multicoverage reflection response of curved interfaces in heterogeneous medium. We compared four traveltime approximations (hyperbolic and non-hyperbolic) of these methods by using synthetic data. This work shows that the Multifocusing method is significantly more accurate than the other traveltime approximations at larger offsets and at larger midpoint separations while using essentially the same number of parameters.

Introduction

Time-domain stacking plays a key role in several model-independent imaging techniques (Hubral, 1999). According Landa et al. (2010) improving the quality of time-domain stacked sections remains the focus of intensive research, in particular toward improving the accuracy of the normal-moveout (NMO) correction.

In the last years, we have found diverse stacking methods as an extension of the conventional imaging method, the Common-midpoint (CMP) stacking. Instead of working only with one kinematic parameter or the stacking velocity (CMP method), the new methods provide two or three parameters for each point of the simulated zero-offset (ZO) section. Examples of such methods are the well known Common-Reflection-Surface (CRS) stack (Jäger et al., 2001) and Multifocusing (MF) stack (Gelchisnky et al., 1997).

The CRS method employs a hyperbolic traveltime approximation (Tygel et al., 1997) that defines a stacking surface for each particular sample in the ZO seismic section to be simulated.

Like the CRS method, the MF method (Landa et al., 2010) considers a collection of traces whose sources and receivers is in a vicinity of the imaging trace (a super-gather), rather than a single CMP gather at a time. This method employs a non-hyperbolic approximation or double-square root formulae (Gelchisnky et al., 1997).

Both MF and CRS use a stacking surface in the mid-point-and-half-offset domain and require estimation of three parameters: the emergence angle of the normal ray (with respect to the measurement surface normal) and the wavefront curvatures of the two hypothetical waves, called Normal-Incidence-Point (NIP) and Normal (N) wave (Hubral, 1983).

Höcht et al. (1999) derived a Taylor expansion of the second-order CRS moveout formula, so-called the fourth-order CRS moveout formula. This new CRS moveout formula is described in terms of the same parameters of the conventional CRS moveout formula.

Chira-Oliva et al. (2003) reviewed the derivation of the fourth-order CRS moveout formula and discussed first comparisons between different seismic configurations with the second-order CRS moveout formula by considering synthetic models. They suggested this high-order moveout formula can provide a better approximation to true traveltimes of reflection or diffraction events than the second-order CRS moveout formula for large offsets. Chira et al. (2010) applied successful both stacking surface approximations in synthetic and real datasets. They shown the fourth-order CRS traveltime generally provides better approximation in larger offset data.

Landa et al. (2010) compared the planar and spherical Multifocusing traveltimes with the second-order CRS traveltime approximation for a range of reflectors with increasing curvature. They shown the planar multifocusing can be remarkably accurate but the CRS becomes increasingly inaccurate.

Fomel and Kazinnik (2012) proposed a non-hyperbolic traveltime approximation to simulate ZO sections. They applied this approximation in synthetic dataset and shown it significantly extends the accuracy range of second-order CRS approximation while using essentially the same set of parameters.

In this work, we tested multiparameter hyperbolic and non-hyperbolic traveltime approximations to simulate ZO sections. We considered the hyperbolic CRS approximations (second and fourth-order), non-hyperbolic CRS approximation and the non-hyperbolic MF approximation. The MF traveltime approximation has shown a better performance to simulate ZO traces when compared with the other approximations.

Methods

We assume that multicoverage data are acquired on a single horizontal seismic line. On this line, we consider a fixed ZO primary reflection ray or central ray. This ray is specified by the coordinate x_0 that locates the coincident source-receiver pair and the start angle β_0 . Paraxial primary reflection rays in the vicinity of the central ray are specified by their midpoint and half-offset coordinates (x_m,h). The traveltime of the two-way ZO central ray is denoted by t_0. The wavefront curvatures, K_N and K_{NIP}, refer to the normal (N) wave and normal-incident-point (NIP) wave, respectively. We assume that the CRS parameters (β_0,K_{NIP},K_N) are known. For a paraxial ray specified by the coordinates (x_m,h), the second-order CRS traveltime approximation (Tygel et al., 1997) is given by

$$t_{2,CRS}^2 = \left[t_0 + \frac{2\sin\beta_0}{v_0}\Delta x\right]^2 + \frac{2t_0\cos^2\beta_0}{v_0}\left[K_N(\Delta x)^2 + K_{NIP}\,h^2\right]. \qquad (1)$$

where $\Delta x = x_m - x_0$.

The fourth-order CRS traveltime approximation (Höcht et al., 1999) is based on the construction of the exact traveltime formula for the case of an inhomogeneous medium where they assumed an emerging wave circular, defined by the emergence angle β_0 and the radius of curvature of the true wave observed at x_0. This wave propagates with a constant velocity v_0 near to the surface. This formula has the form

$$t_{4,CRS}^2 = t_{2,CRS}^2 + \frac{\cos^2\beta_0}{v_0^2}\left[A\Delta x h^2 + B(x_m - x_0)^3 + C(\Delta x)^4 + D(\Delta x)^2 h^2 + Eh^4\right] \qquad (2)$$

where

$$A = 2K_{NIP}\sin\beta_0\left[2 - 2v_0t_0K_N - v_0t_0K_{NIP}\right],$$

$$B = 2K_N\sin\beta_0\left[2 - 2v_0t_0K_N\right],$$

$$C = K_N^2\left[5\cos^2\beta_0 - 4\right]\left[1 - v_0t_0K_N/2\right],$$

$$D = K_{NIP}\left\{2v_0t_0\left[3 - 4\cos^2\beta_0\right]K_N^2 + K_N\left[4 - 5\cos^2\beta_0\right]\left[-2 + v_0t_0K_{NIP}\right] - 2K_{NIP}\sin^2\beta_0\left[2 - v_0t_0K_{NIP}\right]\right\},$$

$$E = K_{NIP}^2\left[2v_0t_0K_N\sin^2\beta_0 - (v_0t_0K_{NIP}\cos^2\beta_0/2) + \cos^2\beta_0\right]$$

Fomel and Kazinnik (2012) proposed a new non-hyperbolic approximation. The form of this approximation follows from an analytical equation for reflection traveltime from a hyperbolic reflector. This approximation is given by

$$t_{NH-CRS} = \sqrt{\frac{F(\Delta x) + ch^2 + \sqrt{F(\Delta x - h)F(\Delta x + h)}}{2}}, \quad (3)$$

where

$$F(\Delta x) = \left[t_0 + \frac{2\sin\beta_0}{v_0}(\Delta x)\right]^2 + \frac{2t_0\cos^2\beta_0}{v_0}\left[K_N(\Delta x)^2\right],$$

$$c = \frac{4t_0\cos^2\beta_0 K_{NIP}}{v_0} + \frac{4\sin^2\beta_0}{v_0^2} - \frac{4t_0\cos^2\beta_0 K_N}{v_0}.$$

The MF method constructs the moveout based on two spherical waves at each source and receiver point, respectively. These two waves are mutually related by a focusing quantity that is a function of the source and receiver location rather than a fixed parameter for a given multicoverage gather (Landa et al., 2010). This expression is given by

$$t_{mult}(x_m, h) = t_0 + \Delta t_s + \Delta t_G \qquad (4)$$

where

$$\Delta t_s = \frac{1}{v_0K_S}\left[\sqrt{1 + 2K_S\sin\beta_0\Delta x_S + (K_s\Delta x_S)^2} - 1\right],$$

$$\Delta x_S = x_s - x_0, \quad K_S = \frac{K_{NIP} - \Gamma K_n}{1 - \Gamma},$$

$$\Delta t_G = \frac{1}{v_0K_G}\left[\sqrt{1 + 2K_G\sin\beta_0\Delta x_G + (K_G\Delta x_G)^2} - 1\right],$$

$$\Delta x_G = x_G - x_0, \quad K_G = \frac{K_{NIP} + \Gamma K_n}{1 + \Gamma},$$

$$\Gamma = \frac{x_m - x_0}{h}.$$

Examples

We considered a model constituted of two homogeneous layers above a half-space. The acquisition is lying on a horizontal line (Figure 1). Based on this model, we generated a synthetic dataset of multicoverage primary reflections, using the ray-tracing algorithm, SEIS88 (Cerveny and Psensik, 1988). The data do not have noise and were created according a common-shot (CS) configuration. The maximum offset was 4 km. The source signal was a Gabor wavelet with 40 Hz dominant frequency and the time sampling was 25ms.

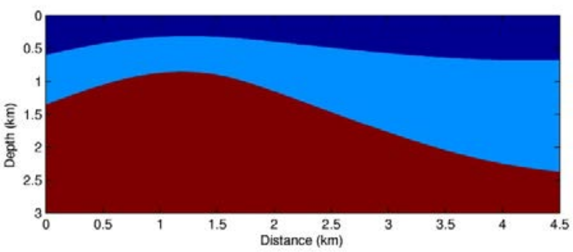

Figure 1. 2-D model constituted of two isovelocity layers about a half-space with curved interface. Interval velocities are 2.5 km/s, 3.0 km/s and 3.5 km/s, respectively.

Figure 2 shows the ray-theoretical modeled ZO section without noise. Figure 3 shows the simulated ZO section that results from the application of the non-hyperbolic CRS traveltime approximation. We also show the differences in amplitudes between the ZO original section and the simulated ZO section by the non-hyperbolic CRS stacking method. Figure 4 shows the simulated ZO section that results from the application of the second-order CRS moveout formula. We show the differences in amplitudes between the ZO original section and the second-order CRS stacking. Figure 5 shows the simulated ZO section that results from the application of the fourth-order CRS moveout formula. We also show the differences in amplitudes between the ZO original section and the fourth-order CRS stacking. Finally, Figure 6 shows the simulated ZO section that results from the application of the non-hyperbolic MF traveltime approximation. It is also shown the differences in amplitudes between the ZO original section and the simulated ZO section by the MF method.

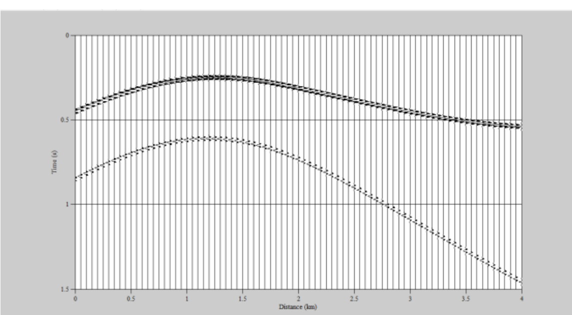

Figure 2. Ray-theoretical modeled ZO section.

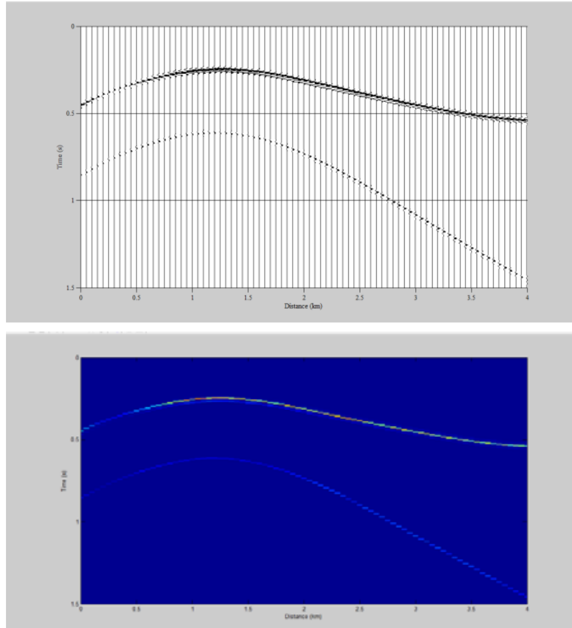

Figure 3: Top: Non-hyperbolic CRS stacking. Bottom: Differences in amplitudes between the ZO original section and the non-hyperbolic CRS stacking.

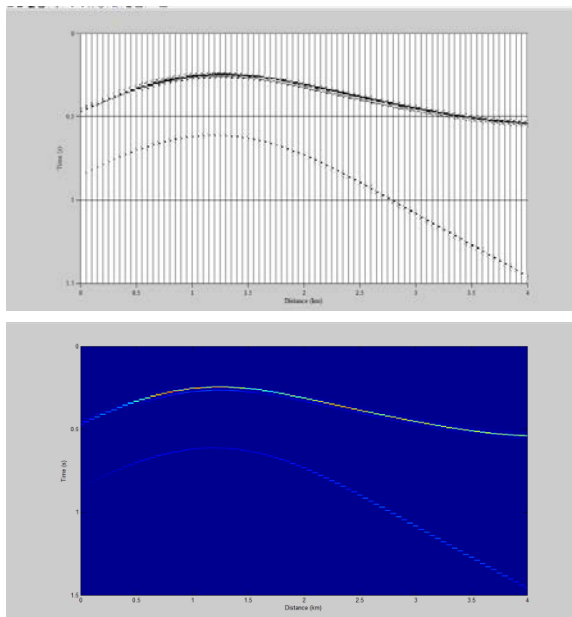

Figure 4: Top: Second-order CRS stacking. Bottom: Differences in amplitudes between the ZO original section and the second-order CRS stacking.

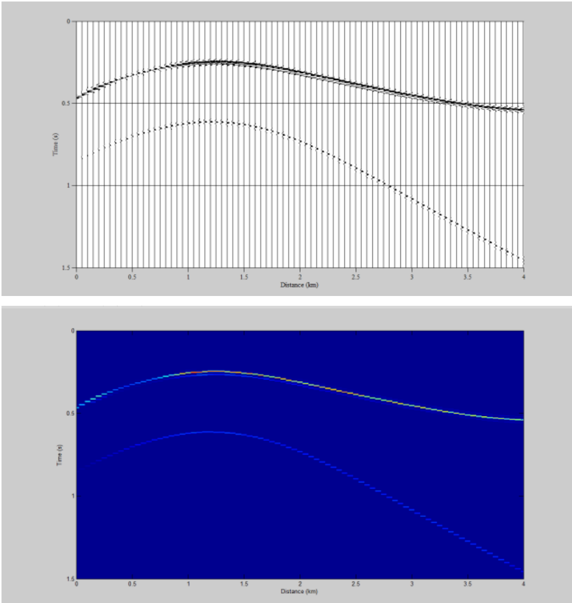

Figure 5: Top: Fourth-order CRS stacking. Bottom: Differences in amplitudes between the ZO original section and the fourth-order CRS stacking.

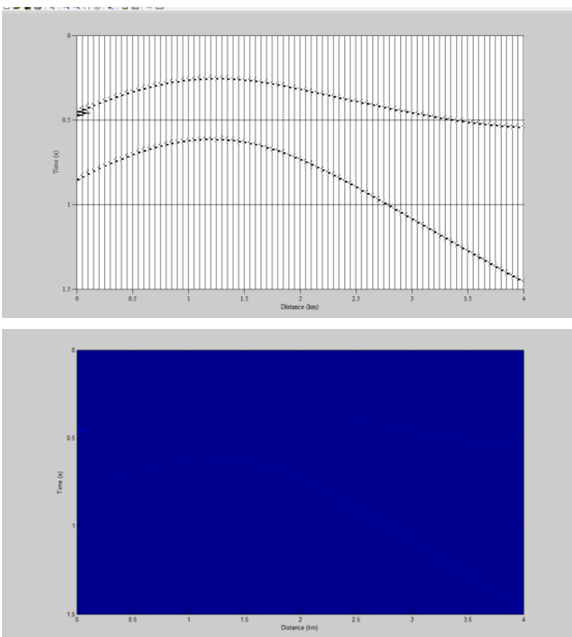

Figure 6: Top: MF stacking. Bottom: Differences in amplitudes between the ZO original section and the MF stacking.

Conclusions

We tested multiparameter hyperbolic and non-hyperbolic traveltime approximations to simulate ZO sections. We considered the second and fourth-order hyperbolic CRS traveltime approximations, non-hyperbolic CRS approximation and the non-hyperbolic MF approximation. The MF traveltime approximation presented a better performance to simulate ZO traces when compared with the other approximations.

Acknowledgments

We thank the sponsors of the Wave Inversion Technology (WIT) Consortium (Germany) for their support and the SW3D Consortium for the SEIS88 software.

References

Cerveny, V. and Psensik, I.,1988. Ray Tracing program. Charles University, Czechoslovakia.

Chira-Oliva, P., Tygel, M., Hubral, P., and Schleicher, 2003. A fourth-order CRS moveout for reflection or diffraction events: numerical examples. *Journal of Seismic Exploration*, **12,** 197–219.

Chira-Oliva, P., Garabito, G., Cruz, J. C. R., 2010. Fourth Order CRS Stacking Method: Examples: 72nd Conference & Exhibition, EAGE, Extended Abstracts, 14-17.

Fomel, S. and Kazinnik, R., 2012. Non-hyperbolic common reflection surface. doi: 10.1111/j.1365-2478.2012.01055.x. Geophysical Prospecting, 1–7.

Gelchisnky, B., Berkovitch, A., and Keydar, S., 1997. Multifocusing homeomorphic imaging: Parts I and II: Course Notes. Special Course on Homeomorphic Imaging, Seeheim, Germany.

Höcht, G., de Bazelaire, E., P., M., and Hubral, P., 1999. Seismic and optics: hyperbolae and curvatures. *Journal of Applied Geophysics*, **42**, 261–281.

Hubral, P. (Ed.), 1999. Macro-Model Independent Seismic Reflection Imaging. *Journal of Applied Geophysics*, **42**, 137–346.

Hubral, P., 1983. Computing true amplitude reflections in a laterally inhomogeneous earth. *Geophysics*, **48**, 1051–1062.

Jäger, R., Mann, J., Höcht, G., and Hubral, P., 2001. Common reflection surface stacking stack: Image and attributes.*Geophysics*, **66**, 97–109.

Landa, E., Keydar, S. And Moser, T. M., 2010. Multifocusing revisited – inhomogeneous media and curved interfaces. Geophysical Prospecting, **58**, 925-938.

Tygel, M., Müller, T., Hubral, P., and Schleicher, J., 1997, Eigenwave based multiparameter traveltime expansions, 67th Ann. Internat. Mtg., SEG, Expanded Abstracts, 1770-1773.